ELSEVIER

Materials Science and Engineering B 126 (2006) 164–167

MATERIALS SCIENCE & ENGINEERING B

www.elsevier.com/locate/mseb

Temperature dependence of spin transport by dynamic quantum dots

J.A.H. Stotz*, R. Hey, P.V. Santos

Paul-Drude-Institut für Festkörperelektronik, Hausvogteiplatz 5-7, 10117 Berlin, Germany

Abstract

Electron spins in an undoped quantum well are transported using dynamic quantum dots (DQDs) formed by the piezoelectric potential of surface acoustic waves. The temperature dependence of the coherence length of electron spins during transport is investigated using spatially resolved photoluminescence. For temperatures between 4.2 and 20 K, the spin coherence length, which is proportional to the spin coherence lifetime, remains constant at approximately 100 μm. This results from the ability of the DQDs to confine the spins within a small area (1 μm × 1 μm to 2 μm × 2 μm) during transport and reduce the temperature dependence associated with D'yakonov-Perel' (DP) spin scattering. At 30 K, the electron spin coherence length rapidly decreases as the DP mechanism becomes dominant because of the higher thermal velocity on the Fermi surface.

Keywords: Surface acoustic waves; Dynamic quantum dots; Spin transport; Photoluminescence

1. Introduction

Spintronic devices based on the manipulation of electron spins are candidates for future generations of faster and lower power electronics as well as for applications in quantum information processing [1]. Semiconductor-based spintronic devices are particularly interesting because of the well-established technology, fundamental research, and understanding behind conventional semiconductor devices. Previous studies concerning spin control in semiconductors have addressed (i) the confinement of spins within a quantum dot to achieve long spin lifetimes at the expense of transport [2] or (ii) the transport of spins over long distances with little control on the microscopic movement of the spin carriers [3]. While each of these systems has yielded interesting results, the combination of the two concepts – long range transport of confined spins – provides new possibilities for spintronic applications.

The combination of long-range transport using confined spin carriers can be realized using specially designed semiconductor electrostatic potentials. Beginning with a simple, undoped GaAs quantum well (QW), two orthogonally propagating surface acoustic wave (SAW) beams are excited. The interference of the piezoelectric fields at the intersection of the two beams produces an array of mobile confinement potentials, referred to as dynamic quantum dots (DQDs), that are able to transport both electrons and holes [4,5]. We have previously demonstrated that an ensemble of optically excited electron spins can be transported by DQDs while maintaining spin coherence over lengths exceeding 100 μm [6]. While the long spin coherence lifetime is attributed to a combination of mesoscopic confinement effects [7] with high local electron densities within the DQDs, [8] the details of the spin scattering mechanisms are not well understood. Here, we address this issue by investigating the effects of temperature on the long-range electron spin transport using DQDs.

2. Experimental setup

A single 20 nm-thick GaAs QW with $Al_{0.3}Ga_{0.7}As$ barriers placed 390 nm below the surface was grown by molecular-beam epitaxy on a GaAs (0 0 1) semi-insulating substrate. In the absence of a SAW, the photoluminescence (PL) from the electron–heavy hole transition of the QW was centred at 813.5 nm with a spectral width less than 0.2 nm. The DQDs were formed as a result of the interference of two orthogonally propagating SAW beams, as shown in Fig. 1 [4,5]. The 120 μm wide plane waves, each with a wavelength λ_{SAW} of 5.6 μm and a linear power density of approximately 7 W/m, were generated by exciting a linear array of aluminum interdigitated transducers (IDTs) that were deposited on the sample's surface. The SAWs propagate along the $x' = [1\,1\,0]$ and $y' = [1\,\bar{1}\,0]$ surface directions with a well-defined phase velocity $v_{SAW} = 2907$ m/s. Over the range of temperatures studied here, v_{SAW} varies less than 0.1%. The corresponding SAW frequency is $\omega_{SAW}/2\pi = 519$ MHz at a tem-

* Corresponding author.
E-mail address: jstotz@pdi-berlin.de (J.A.H. Stotz).

0921-5107/$ – see front matter © 2005 Elsevier B.V. All rights reserved.
doi:10.1016/j.mseb.2005.09.038

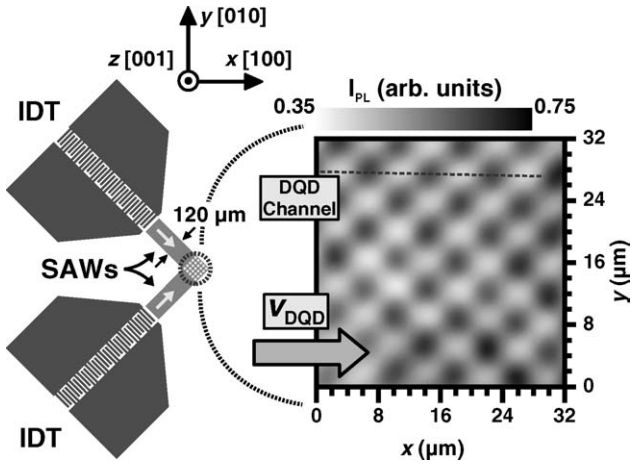

Fig. 1. Schematic diagram of the formation of DQDs. Two SAW beams propagate out of the IDTs and travel along the [1 1 0] and [1 $\bar{1}$ 0] directions on the (0 0 1) GaAs surface. The interference of the SAW beams generates the DQD array. The expanded view shows a time-resolved PL image of the DQD array at a particular phase of the SAWs. Regions of high (low) PL intensity correspond to the position of DQDs that confine the electrons (holes). The dotted line represents the channel along which one row of DQDs propagate. The sample temperature was 12 K.

perature of 12 K. The type-II piezoelectric field generated by the SAW interference confines the electrons and holes within an array of DQDs, each of dimensions between 1 μm × 1 μm and 2 μm × 2 μm. The DQD array propagates along the [1 0 0] direction with a velocity $v_{DQD} = \sqrt{2}v_{SAW}$ and has a periodicity $\lambda_{DQD} = \sqrt{2}\lambda_{SAW}$.

A schematic of the experimental setup used for the spin-sensitive, spatially dependent PL studies is shown in Fig. 2. The sample was mounted in a temperature-controlled, optical He-flow cryostat equipped with special feed-throughs for the rf excitation of the IDTs. The carriers were photogenerated at position G using a continuous wave (cw) Ti:sapphire laser with a wavelength of 768 nm. The incoming laser beam was circularly polarized using a λ/4 plate and, using a microscope objective, focussed to a spot with a diameter of approximately 5 μm leading to an optical power density of approximately 0.1 μW/μm^2. The PL was collected by the same objective and passed through an acousto-optic modulator (AOM) and a λ/4 plate. A polarizing beam displacer was inserted to spatially separate the paths of right (I_R) and left (I_L) polarizations of the PL. To spectrally select the electron–heavy hole transition, a band-pass filter with a centre wavelength of 810 nm and a spectral width of 20 nm was used. The two polarization images were then focussed onto separate regions of an intensified charge-coupled device (ICCD). Because of the polarization dependence of the components along the optical path, I_R and I_L were calibrated through the use of the AOM. When the AOM is turned on, it modulates the polarization of the PL such that the time-averaged signal is unpolarized and can thus be used as a reference. When the AOM is off, the circular polarization of the incident laser light creates spin-polarized electrons and holes at G. Holes are excited from both valence bands, which experience rapid spin decoherence through hole-spin scattering as they thermalize. The degree of circular

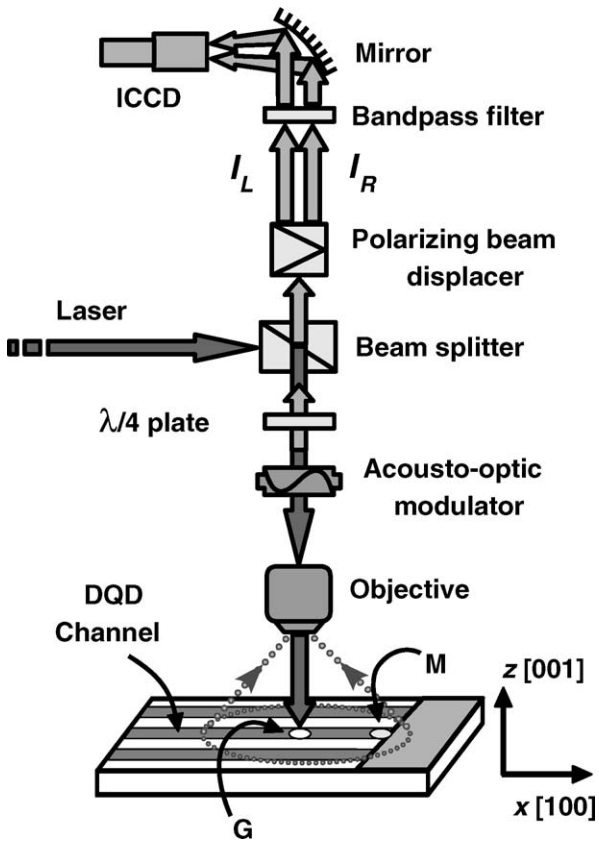

Fig. 2. Schematic for the optical detection of spin transport. A cw laser beam passes through the λ/4 plate to become circularly polarized and is focussed by an objective to a small spot G on the sample. Photogenerated electrons and holes are transported along the DQD channel towards a semi-transparent metal strip M, where they recombine. Light is collected by the objective from the surrounding area, including the luminescence near M. The circularly polarized luminescence is converted into linear polarized light by the λ/4 plate. A polarizing beam displacer produces two beams, I_R and I_L, which have intensities proportional to the right- and left-circularly polarized components of the luminescence, respectively. These two polarizations are simultaneously imaged by different areas of an ICCD camera.

polarization of the PL $\rho_z = (I_R - I_L)/(I_R + I_L)$ is, therefore, a suitable measure of the net population of spin-polarized electrons $\rho = (I_\uparrow - I_\downarrow)/(I_\uparrow + I_\downarrow)$.

3. Results and discussion

The area of the DQD array can be imaged using a stroboscopic PL measurement. To generate the image shown in Fig. 1, the sample was uniformly illuminated over the entire field of view with a cw laser beam, and the PL was detected by synchronizing a 300 ps gate of the ICCD with the frequency of the SAWs. A high optical excitation intensity was used to photogenerate a large density of charge carriers, which partially screened the piezoelectric field from the DQDs. Therefore, under these conditions, the photogenerated carriers are not efficiently transported. As Fig. 1 demonstrates, PL of the DQD array reveals a checkerboard pattern, which is very regular and extends for many periods in both directions, comprised of regions with high and low PL intensity corresponding to DQDs